Scaling of Wall Shear Stress Fluctuations in a Turbulent Duct Flow

D.A. Shah* and R.A. Antonia†
University of Newcastle, Newcastle, Australia

Instantaneous fluctuations of the wall shear stress have been measured in a fully developed turbulent duct flow over a factor of 10 variation in the Reynolds number. Distributions for the average frequency of detections obtained using the variable-interval time averaging technique suggest that scaling on outer variables or perhaps a mixture of outer and inner variables is more appropriate than scaling on inner variables when the Reynolds number is sufficiently large. The Reynolds number behavior of the average frequencies of zero crossings and local maxima of the shear stress fluctuation rules out the possibility of outer scaling and indicates a weak Reynolds number dependence when scaled on inner variables. These apparently conflicting trends are discussed in the context of published results on the scaling of wall shear stress fluctuations.

Nomenclature

A,B,n = calibration constants
d = duct half-width
E = instantaneous voltage
$\bar{E}$ = average value of voltage
f_0 = average zero-crossing frequency ($\equiv T_0^{-1}$)
f_1 = average frequency of local maxima of instantaneous shear stress fluctuation ($\equiv T_a^{-1}$)
f_a = average frequency corresponding to the second zero crossing of the autocorrelation of instantaneous shear stress fluctuation ($\equiv T_a^{-1}$)
f_c = low-pass cutoff frequency
f_v = average number of VITA detections per second ($\equiv T_v^{-1}$), see Fig. 2
k = threshold factor
ℓ = sensor length
L = streamwise extent of the film or diameter of the wire
R_d = Reynolds number based on duct half-width ($=U_0 d/\nu$)
R_δ = Reynolds number based on boundary-layer thickness ($=U_1\delta/\nu$)
R_θ = momentum thickness Reynolds number ($=U_1\theta/\nu$)
t = time
T = integration time used in VITA
u = instantaneous velocity fluctuation
U = local mean velocity
U_0 = mean velocity at the duct centerline
U_1 = boundary-layer freestream velocity
U_τ = friction velocity ($=\bar{\tau}/\rho)^{1/2}$
x = streamwise distance from the duct entrance
y = distance normal to the wall
δ = boundary-layer thickness (distance from wall at which $U=0.99U_1$)
θ = momentum thickness $=\int_0^\infty(\rho U/\rho_1 U_1)(1-U/U_1)\mathrm{d}y$
λ = Taylor microscale in time $[=\overline{\alpha^2}/\overline{(\partial\alpha/\partial t)^2}]^{1/2}$, where α is a fluctuating quantity
Λ = zero-crossing time scale ($=1/\pi f_0$)
ν = kinematic viscosity of fluid
σ = molecular Prandtl number of fluid
τ = instantaneous wall shear stress fluctuation
$\bar{\tau}$ = average value of wall shear stress
$\langle\ \rangle$ = conditional average, defined in Eq. (3)
$(\ )^+$ = normalization by inner variables ν and U_τ
$(\ )'$ = rms value of fluctuation, centered about its average value
$(\tilde{\ })$ = low-pass filtering, used for VITA, defined in Eq. (2)

Introduction

IT is well accepted that the bursting phenomenon plays a major role in transports of mass, heat, and momentum and in the production of turbulent energy in turbulent boundary-layer and duct flows. However, significant controversy surrounds the scaling of the frequency of bursting, the latter being identified with the complete cycle of events as described by Kim et al.[1] The bursting frequency has been obtained by a wide range of techniques in different turbulent flows. For example, Narahari Rao et al.[2] found that the average frequency of pulses, identified from band-pass filtered velocity fluctuations, scaled on the outer variables U_1 and δ. Blackwelder and Haritonidis[3] found that the average frequency f_v of detections obtained by the variable-interval time averaging technique (VITA) scaled on inner variables U_τ and ν. Alfredsson and Johansson[4] found that f_v scaled on neither the inner nor outer variables, but rather on the geometric mean of the inner and outer variables. These latter measurements were made in a turbulent duct flow, whereas those of Narahari Rao et al.[2] and Blackwelder and Haritonidis[3] were for a turbulent boundary layer.

There is little evidence to suggest that the different trends may be associated with the different flows. In any case, Blackwelder and Haritonidis[3] suggested that inner scaling applies to both duct and boundary-layer flows, whereas Narahari Rao et al.'s[2] outer scaling in a boundary-layer result was found to apply to a duct flow.[5] Perhaps the main reason for the opposite trends is the inability of different conditional techniques, usually applied to information obtained at only one point in the flow, to detect the bursting phenomenon correctly.[6-8] Although the need for calibrating one-point techniques remains, there are at least two other difficulties that have to be overcome before the question of scaling can be resolved.

The primary difficulty is the need for experiments to cover a sufficiently large range of Reynolds numbers. Reynolds number similarity is not usually reached until a certain Reynolds number is exceeded and may only be achieved asymptotically at infinitely large Reynolds numbers.[9] In a

Received July 1, 1985; revision received Feb. 26, 1986.

*Postgraduate Student, Department of Mechanical Engineering.
†Professor, Department of Mechanical Engineering.

boundary layer, the Reynolds number effects on the outer layer (as reflected, for example, by the strength of the "wake"[10] or by properties of the large-scale structure[11,12]) do not disappear until R_θ exceeds a certain value, somewhere between 3000 and 5000. There is also evidence[13,14] that properties of the outer region of a fully developed turbulent duct flow do not become independent of the Reynolds number until a certain Reynolds number is exceeded. In this sense, it is surprising that the possibility of "low Reynolds number effects" has been ignored in scaling investigations.[3,15]

Another difficulty, not completely unrelated to the previous one, may be the inadequate spatial resolution of sensors used in the detection process. For example, Blackwelder and Haritonidis[3] noted that only sensors with $\ell^+ \leq 20$ were free from spatial averaging effects. This effect appears[14,16] to be largest in the buffer layer, reflecting the importance of ejections (rapid motion of fluid away from the wall) with relatively small spanwise length scales in this region. Closer to the wall, inside the viscous sublayer, sweeps (faster moving fluid toward the wall) with larger spanwise length scales are more important and spatial resolution effects seem to be less important. Offen and Kline[6] noted that, as the fluid motion past a fixed point near the wall due to a low-speed streak is noticeably slower than the local mean velocity for a detectable amount of time, the temporal behavior of a single sensor should be a reliable indicator of spatially coherent events. Chambers et al.[17] exploited this by using a flush-mounted hot-film sensor as a wall shear stress probe to determine f_v in a duct flow. They found that scaling on inner variables was more appropriate than scaling on outer variables over the Reynolds number range $2.6\times10^3 \lesssim R_d \lesssim 1.3\times10^4$.‡ This result is in conflict with the boundary-layer observations[18] that the period T_a, obtained with a hot wire mounted flush with the wall, scales on outer variables. It is also in conflict with the result, in a turbulent duct flow,[19] that the zero-crossing frequency f_0 of the wall shear stress fluctuation tends to scale on outer variables for asymptotically large values of the Reynolds number.

Recently, Badri Narayanan et al.[15] considered wall shear stress fluctuations in a turbulent boundary layer over the range $1000 \lesssim R_\theta \lesssim 5500$ and found that f_0 scaled on outer variables over the complete range of R_θ. However, they noted that f_1, the average frequency of local maxima of τ (these authors called f_1 the "average frequency of fluctuations"), scaled on inner variables.

The main aim of the present measurements was to shed some light on the conflicting trends for f_v, f_1, f_0, and f_a determined from wall shear stress fluctuations. It was important that the measurements covered as wide a Reynolds number range as possible and that the bursting frequency be obtained by several different techniques using different sensor lengths to assess the influence of spatial resolution in the same flow. Accordingly, estimates of f_v, f_1, f_0, and f_a were obtained from wall shear stress fluctuations measured in a turbulent duct flow using two different sensor lengths over a factor of 10 variation in R_d (3300–33,000).

Experimental Details and Conditions

The duct used for the measurements formed the working section of an open-circuit type of blower tunnel, as described in Shah et al.[14] The duct has a length of 7.32 m, a height of 0.76 m, and a width of 42 mm. One of the vertical walls of the duct is made of 19 mm thick Perspex panels. The other wall is made of 11 mm thick aluminum panels. For the present measurements, the wall shear stress probe, described below, was mounted flush with the Perspex wall at a distance $x = 195d$ from the duct entrance. The inlet boundary layers were tripped at $x = 40$ mm with 1.6 mm diameter rods spanning the full height of the duct. Previous hot-wire measurements[14] indicated that the flow is fully developed at the measurement station over the range $3300 \lesssim R_d \lesssim 33{,}000$.

To avoid possible difficulties with the complex low-frequency characteristics of a hot film associated with the thermal interaction between film and supporting substrate,[20] a hot wire, mounted very close to the surface, was preferred to a flush-mounted hot film. Advantages of the wire over the film have already been noted.[21,22] The hot wire was mounted (Fig. 1) on a machined Perspex plug; two holes, 5 mm apart, of 0.8 mm diameter were drilled in the plug and jewellers' broaches were then inserted in the holes. The tips of the broaches were adjusted to be flush with the plug surface before filling the holes with epoxy cement. A pre-etched Wollaston wire was placed on the surface of the plug and soft soldered to the tips of the broaches. It was ensured, by viewing under a microscope, that the wire was straight, just touching the surface. Most of the measurements were made with a 5 μm (Pt/10%Rh) wire of length $\ell \simeq 0.7$ mm. A few measurements were made with a 2.5 μm (Pt) wire of length 0.38 mm. The Perspex plug-wire assembly was then fitted to one of the removable Perspex plugs used in the duct working section. The frequency response of the plug-wire assembly/DISA 55M10 circuit was checked using the square-wave technique (e.g., at $R_d \simeq 7000$, the -3 dB frequency was estimated to be about 25 and 30 kHz for the long and short wires, respectively). The wall probe was calibrated in situ, $\bar{\tau}$ in the duct being determined from either the mean static pressure gradient or a Preston tube. Agreement between the latter two estimates of $\bar{\tau}$ was within $\pm 5\%$. The calibration constants A, B, and n

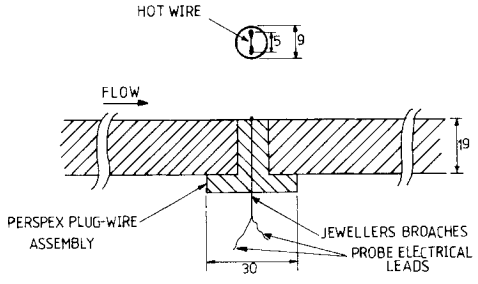

Fig. 1 Schematic arrangement of the wall shear stress gage (all dimensions in millimeters).

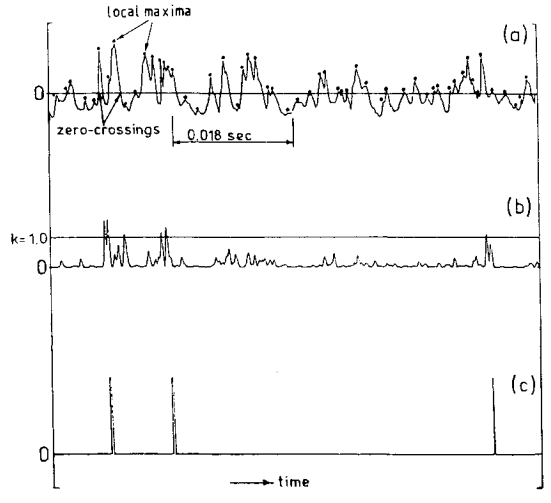

Fig. 2 Typical sample of wall shear stress fluctuation τ and the corresponding VITA variance and detection output ($R_d \simeq 17{,}100$): a) fluctuation τ; b) VITA variance function for $T^+ \simeq 13$; c) VITA detections for $k = 1.0$. There are 48 zero crossings ($f_0 \simeq 657$ Hz), 55 local maxima ($f_1 = 753$ Hz) and 3 VITA detections ($f_v = 41$ Hz).

‡The Reynolds numbers quoted by these authors were based on the hydraulic diameter and the bulk velocity. They have been converted to R_d using Dean's[13] empirical relations.

in $\bar{E}^2 = A + B\bar{\tau}^n$ were determined from a least-squares fit to the calibration points. Calibrations, carried out on different days, yielded values of n in the range 0.68–0.73. These values were significantly higher than the value of 0.33 usually quoted for a wall-mounted hot-film probe. Spence and Brown[23] showed that, for a wall shear stress gage, a necessary requirement for $n = 0.33$ is $U_\tau L/\nu > 6.6/\sigma^{1/2}$. This requirement is not satisfied for the present probe and experimental conditions ($U_\tau L/\nu \simeq 0.43$–3.23). The effect of thermal conduction from the hot wire to the wall is small due to the combination of the relatively low thermal conductivity of the Perspex wall and the small overheat of the wire. In any case, the in situ calibration of the wire should inherently account for the transfer of heat from the wire to the wall.

The probe was operated at a constant temperature in a DISA 55M10 circuit. Most of the measurements were made at an overheat ratio of 0.2, although a few measurements were also made with overheat ratios of 0.1 and 0.3. The effect of overheat was not noticeable for the present measurements. After offsetting the dc voltage from the anemometer, the fluctuating voltage was amplified and recorded on an FM tape recorder (HP3960) at 38.1 cm/s. Records of about 60 s were digitized using an 11 bit + sign A/D converter, at sampling frequencies selected in the range of 2.5–12 kHz, depending on the particular Reynolds number used. Prior to digitizing, the signal was low-pass filtered using a Krohn-Hite filter. For a particular R_d, the filter cutoff frequency f_c was selected such that f_c exceeded the value at which the zero-crossing frequency f_0 became constant. A sampling frequency equal to $2f_c$ was used. The extent of this plateau decreased with increasing R_d, as previously noted by Sreenivasan and Antonia.[19] By assuming the validity of the relation[24] $E^2 = A + B\tau^n$, the values of A, B, and n being those determined by calibration, the time series for the fluctuating voltage was converted into a time series for τ. Statistics of τ, relative to $\bar{\tau}$, were then computed using a PDP 11/34 computer.

Results and Discussion

Root mean square values of τ, viz. τ', obtained with the long wire are shown in Table 1. Also included in this table is U_τ and ℓ^+. The ratio $\tau'/\bar{\tau}$ is essentially constant except for the smallest value of R_d where a slight decrease in relative intensity is observed. Such a decrease was also observed[14] in the ratio u'/U_τ measured at $y^+ \simeq 15$ and was interpreted to reflect a reduction in relative intensity of the large-scale motion of the flow.

The magnitude of $\tau'/\bar{\tau}$ compares favorably with previously published data. For example, Eckelmann[25] reported a value of 0.24 at Reynolds numbers of 2800 and 4100 in a turbulent duct flow. Sreenivasan and Antonia[19] obtained 0.25, also in a turbulent duct flow, over the range $6\times10^3 \lesssim R_d \lesssim 1.2\times10^4$. Kreplin and Eckelmann[26] obtained 0.25 for $R_d \simeq 3900$. Thomas[27] obtained 0.22 in a turbulent boundary layer over the range $6.7\times10^3 \lesssim R_\delta \lesssim 10.1\times10^3$. Badri Narayanan et al.[15] do not report values for $\tau'/\bar{\tau}$, while Chambers et al.[17] present unusually low values in the range 0.057–0.065 (it is unlikely that they were caused due to a high-pass cutoff frequency of 0.1 Hz). The reason for these low values is not clear.

In Chambers et al.'s[17] experiment, ℓ^+ was in the range 22–98. For Badri Narayanan et al.'s[15] experiment, ℓ^+ was estimated, using information given in Badri Narayanan et al.[28] to be in the range 32–153. The average spanwise spacing of low-speed streaks is about[29] 100 viscous lengths (1 viscous length is equal to the ratio ν/U_τ), independent of Reynolds number. The average spanwise distance between low- and high-speed streaks would appear[30] to be of order 50 viscous lengths. Smith's[31] observations suggest that the spanwise extent of energetic near-wall eddies may be several times their streamwise extent, typical estimates for the latter ranging 20–40 viscous lengths.[32] These considerations would suggest

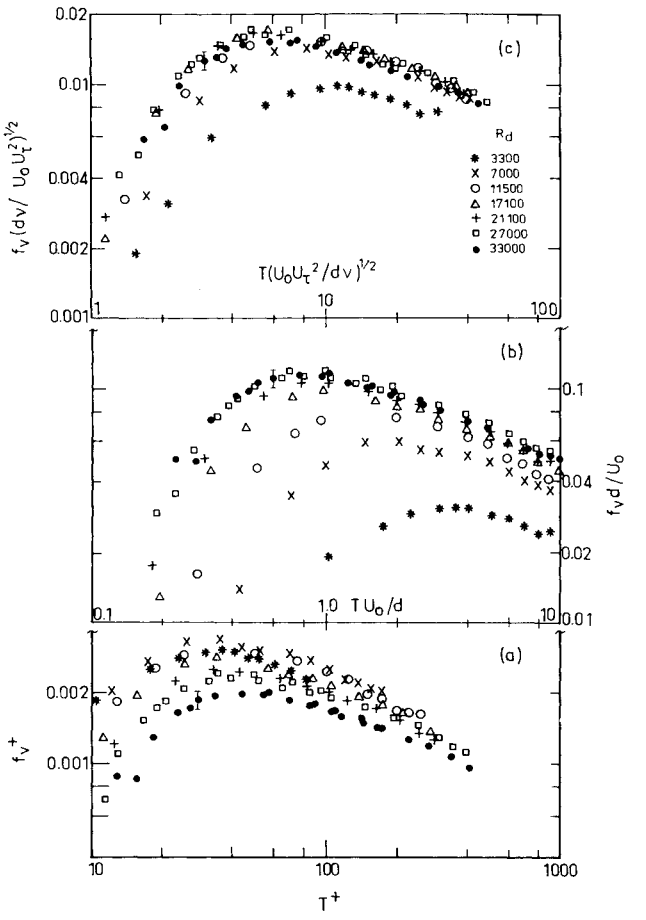

Fig. 3 Dependence of the VITA detection frequency on the integration time T: a) wall scaling; b) outer scaling; c) mixed scaling (vertical bar | indicates maximum uncertainty).

Table 1 Statistics of wall shear stress fluctuations

U_0,m/s	U_τ,m/s	R_d	ℓ^+	$\tau'/\bar{\tau}$	$\tau'/U_0^2\times10^4$
2.4	0.13	3,300	6.1	0.23	7.4
5.0	0.25	7,000	11.7	0.27	6.31
8.2	0.39	11,500	18.2	0.29	6.06
12.2	0.55	17,100	25.7	0.29	5.57
15.1	0.67	21,100	31.3	0.29	5.31
19.3	0.83	27,000	38.7	0.28	5.05
23.3	0.97	33,000	45.3	0.27	4.63

that statistics obtained with wall shear stress probes with a spanwise extent greater than about 40 viscous lengths will be affected by spatial averaging. Johansson and Alfredsson's[16] results for u' tend to indicate that the spatial averaging effect on u' becomes less important as the sublayer is approached; however, data for different ℓ^+ are not shown for $y^+ \lesssim 5$, so that it would be difficult to extrapolate these results to $y = 0$. It is also not possible[17] to extrapolate to $y = 0$ the observation of Blackwelder and Haritonidis,[3] made at $y^+ \simeq 15$, that f_v is reduced for $\ell^+ \gtrsim 20$.

In light of previous considerations, measurements of τ were made with a short wire so that ℓ^+ was in the range 3–25 over the full range of R_d. The values of $\tau'/\bar{\tau}$ agreed, to within $\pm 4\%$, with those shown for the longer wire in Table 1. This result is at variance[14,16,33] with the measured influence of ℓ^+ on u', measured at $y^+ \simeq 15$, and suggests that spatial resolution effects are not as important within the viscous sublayer as at $y^+ \simeq 15$. The observed independence of $\tau'/\bar{\tau}$ with ℓ^+, over the present range of ℓ^+, is in agreement with the notion that the viscous sublayer is dominated by

sweeps that have been observed (e.g., Ref. 32) to have larger spanwise extents than ejections. Consequently, spatial averaging effects are less important at the wall than at $y^+ \simeq 15$. This is consistent with the conclusion, based on measurements[14,16] of the probability density function of u at several values of y^+, that spatial resolution effects on u' and higher-order moments of u become less important as sublayer is approached.

VITA has been applied to the shear stress fluctuations in similar fashion to Chambers et al.[17] A detailed description of the method was given by these authors and the original users[34] of the method. It is sufficient to recall that the output D of the detection algorithm is unity when the following conditions are satisfied:

$$\tilde{\tau}^2 - \bar{\tau}^2 > k\tau'^2 \tag{1a}$$

$$\frac{\partial \tau}{\partial t} > 0 \tag{1b}$$

and is zero for other values of the digital time series.

The tilde represents a low-pass filtering operation with a cutoff at T^{-1}, viz.,

$$\tilde{\tau}(t,T) = T^{-1} \int_{t-T/2}^{t+T/2} \tau(s)\,ds \tag{2}$$

where τ is understood here to be taken with respect to its mean value. The second condition was included, as in the case of Chambers et al.[17] and Blackwelder and Haritonidis[3] (VITA was applied to u at $y^+ \simeq 15$), to focus the detection on events with positive acceleration, presumably associated with the occurrence of a sweep at the probe location. The frequency with which the above detection criteria are satisfied is identified with $f_v (\equiv T_v^{-1})$. The magnitude of f_v depends critically on the choices of the threshold k and averaging time T. We have used the same value of $k(=1)$ selected in previous studies.[3,4,14] Chambers et al.[17] used a much lower value of $k(=0.3)$ to increase the number of detections and improve the sensitivity to the total signal. This was not considered necessary for the present investigation. We established that f_v decreases exponentially with increasing k as in the case of velocity fluctuations.[14,35] We also noted that the normalization used by Blackwelder and Kaplan[34] to collapse ensemble averages of u for different values of k was applicable to $\tau (k \simeq 0.3-2.5)$. Therefore, it seemed justifiable to retain the same values of k for the analysis of shear stress fluctuations. Note that a duration of 60 s was sufficient for determining stable values of f_v.

A short segment of the wall shear stress fluctuations is shown in Fig. 2a and the corresponding normalized variance function $(\equiv \tilde{\tau}^2 - \bar{\tau}^2/\tau'^2)$ and the output D of the detection algorithm for the selected values of T and k are shown in Fig. 2b and 2c, respectively.

Johansson and Alfredsson[35] recommended that, when investigating the scaling of the duration of VITA events, it was important to consider the distribution of f_v for various values of T since the duration of the detected event is closely related to T. We have followed this recommendation and distributions of f_v are shown in Fig. 3 for the three types of scaling over a wide range of T.

The distributions of Fig. 3 have a tendency to collapse at relatively large Reynolds numbers when the scaling is on either the outer or mixed variables. The use of mixed variables brings out a collapse at a smaller Reynolds number ($R_d \gtrsim 11{,}500$) than indicated by outer scaling ($R_d \gtrsim 21{,}100$). There is no suggestion of an approach toward a universal distribution when inner scaling is used. We also ascertained that the distributions at the largest values of R_d were not affected by wire length since the distributions obtained with the short wire were identical to those shown in Fig. 3. The most probable value of f_v occurs at $TU_0/d \simeq 0.8$ or $T(U_\tau^2 U_0/\nu d)^{1/2} \simeq 6$. For comparison, Johansson and Alfredsson[35] obtained a collapse only on mixed variables and their most probable value of f_v occurred at $T(U_\tau^2 U_0/\nu d)^{1/2} \simeq 5$ for $y^+ \simeq 6$.

Chambers et al.[17] (also Blackwelder and Haritonidis[3]) considered the variation of f_v with Reynolds number for only one particular value of T, viz. $T^+ \simeq 10$. The present distributions for a particular value of $T^+ (= 13)$ are shown in Fig. 4. Clearly, the conclusions that can be drawn from this figure do not differ from those drawn in Fig. 3, although the use of only one particular value of T^+ can result in a more ambiguous interpretation of the data than is possible when the results for all values of T^+ are available (Fig. 3). The magnitude of f_v^+ continues to decrease systematically as R_d increases, undermining previous suggestions[3,17] that inner scaling is more appropriate than outer scaling. It has been suggested[36] that the use of a particular value of T normalized with inner variables may bias the outcome. We found that normalizing T with either outer or mixed variables did not alter the result. In each case, f_v scaled better on outer or mixed variables than on inner variables.

It is difficult to decide between outer and mixed scaling as the most appropriate choice. Such a decision would require independent evidence of the Reynolds number dependence of the large structure of the flow. The best evidence we have[14] that such a dependence is real and should not be overlooked when searching for an appropriate scaling is that such Reynolds number effects are evident on distributions of $f_v d/U_0$ vs TU_0/d obtained with a hot wire located in the outer part of the duct, e.g., at $y/d = 0.3$ or 0.5.

It is of interest to briefly examine the VITA conditional averages, viz., the average signature of the events detected by the VITA technique. Conditional averages of τ are obtained, subsequent to the identification of the detection instants t_n, using

$$\langle \tau(t) \rangle = N^{-1} \sum_{n=1}^{N} \tau(t_n + t) \tag{3}$$

where N is the total number of detections. The value of N used to obtain the conditional averages varied 150–1500 over the range of R_d. Note that $\langle \tau \rangle$ contains information about the amplitude of VITA events; therefore, it is not surprising that the distributions (Fig. 5a) of $\langle \tau \rangle / \bar{\tau}$ vs tU_τ^2/ν are essentially independent of R_d since $\nu'/\bar{\tau}$ is essentially independent of R_d. When outer variables are used (Fig. 5b), the maximum value of $\langle \tau \rangle / U_0^2$ decreases with R_d; at the largest Reynolds numbers, the trend is toward a unique distribution, reflecting the declining rate of U_0/U_τ as R_d increases. The conditionally averaged distributions in Fig. 5 are in qualitative agreement with those presented in a duct[17] and in a boundary layer.[27,37] It can be seen that $\langle \tau \rangle$ is almost constant before the sudden increase at $t = 0$ (the detection instant), while the return of $\langle \tau \rangle$ toward an undisturbed state is rather slow.

The accuracy of zero-crossing frequency measurements can be significantly influenced by various factors, such as the dynamic range of the signal, the discriminator characteristics, the filter frequency, and the possibility of noise contamination. Sreenivasan et al.[38] discussed the dead-band effect of their analog comparator, the comparator output being triggered only when the signal level crosses this dead band. In the present measurements, counting was carried out on the computer, but the influence of an effective dead band of amplitude k_1 on the number of crossings was examined at various Reynolds numbers. A crossing was deemed to occur only when the full width of this band was crossed. When the crossing frequency is plotted as a function of k_1, a significant plateau was obtained near $k_1 = 0$ at all Reynolds numbers. Typically, the width of the plateau was about $0.4\tau'$. The signal-to-noise ratio was also checked by examining the effect of the filter cutoff frequency on f_0. A significant plateau was

found, as in the experiments of Sreenivasan and Antonia[19] and Sreenivasan et al.[38], suggesting that the signal-to-noise ratio was adequate.

The magnitude of T_0U_0/d continues to decrease as R_d increases (Fig. 6b) and exhibits a rather strong Reynolds number dependence ($\sim R_d^{-0.59}$). This result is in agreement with the findings of Sreenivasan et al.[38] based on several measurements of f_0 for $y^+ \lesssim 3$, that $T_0U_0/d \sim R_\theta^{-0.7}$. It is in conflict with Badri Narayanan et al.'s[15] finding that f_0 scales on outer variables and an earlier speculation by Sreenivasan and Antonia[19] that T_0U_0/d may become constant at asymptotically large Reynolds numbers.

Present measurements at $y^+ \simeq 15$ and at $y/d = 0.5$ confirmed the strong Reynolds number dependence of T_0U_0/d. This result is consistent with the equality between the zero-crossing time scale Λ and the Taylor microscale λ (in time), irrespective of location in the flow. The observed dependence of T_0U_0/d on R_d in the outer layer ($\sim R_d^{-0.45}$) is consistent with a $R_d^{-1/2}$ variation for $\bar{\lambda}/d$ (where $\bar{\lambda} = U\bar{\lambda}$, assuming Taylor's hypothesis to be valid) if we assume that production and dissipation of turbulent energy are approximately equal. All the previous observations corroborate the conclusion by Sreenivasan et al.[38] that the zero-crossing length scale contains no more information than the Taylor microscale.

The weak dependence in Fig. 6a of $T_0U_\tau^2/\nu$ on R_d ($\sim R_d^{0.17}$) also corroborates Sreenivasan et al.'s[38] relation $T_0U_\tau^2/\nu \sim R_\theta^{0.12}$, established over a wider range of R_θ. It is worth briefly recalling the physical, although perhaps oversimplified, explanation offered by these authors. Since a large number of zero crossings is associated with small-scale fluctuations, which are viscosity dependent, the zero-crossing frequency should scale, to a large degree, on inner variables. The weak R_d dependence is no doubt due to a small number of longer intervals associated with large structures.

The average frequency f_1 was determined by counting the number of local peaks on computer plotted traces of τ, such as shown in Fig. 2a. The magnitude of f_1 is usually, but not always, slightly ($\simeq 10\%$) larger than f_0, but the Reynolds number variation of f_1 is essentially identical to that of f_0 and consequently the scaling trends established for f_0 are applicable to f_1. This contrasts with Badri Narayanan et al.'s[15] finding that f_0 scales on outer variables, whereas f_1 scales on inner variables. The average frequency f_1 has also been inferred from Eckelmann's[25] traces of τ (Fig. 4 of Ref. 25) in a turbulent duct flow for three relatively small values of R_d. Eckelmann's[25] values are also shown in Fig. 6b, the error bar for these data representing the maximum variation in these quantities inferred from the determination of f_1 on the basis of 10 separate records of τ (Fig. 6 of Ref. 25) at $R_d \simeq 4100$. The agreement between the present results and those of Eckelmann[25] is reasonable considering the relatively short record duration and small Reynolds numbers in Ref. 25.

Laufer and Badri Narayanan[18] estimated T_a from the long-time autocorrelation of signals from a hot wire mounted flush with the wall. More precisely, the extent of the second zero, corresponding to the end of the negative portion of autocorrelation curve was used to represent T_a. The average period T_a was found to scale on the outer variables ($1800 < R_\theta < 6000$) with $T_aU_1/\delta \simeq 5$ and $T_a^+ \simeq 0.65\, R_\theta^{0.75}$. It should be noted that a precise determination of T_a from the autocorrelation curve is difficult due to its wavy nature. In the present investigation, the curves were smoothed to estimate T_a. The measurements of T_a for $R_d \gtrsim 7000$ qualitatively support the conclusion of

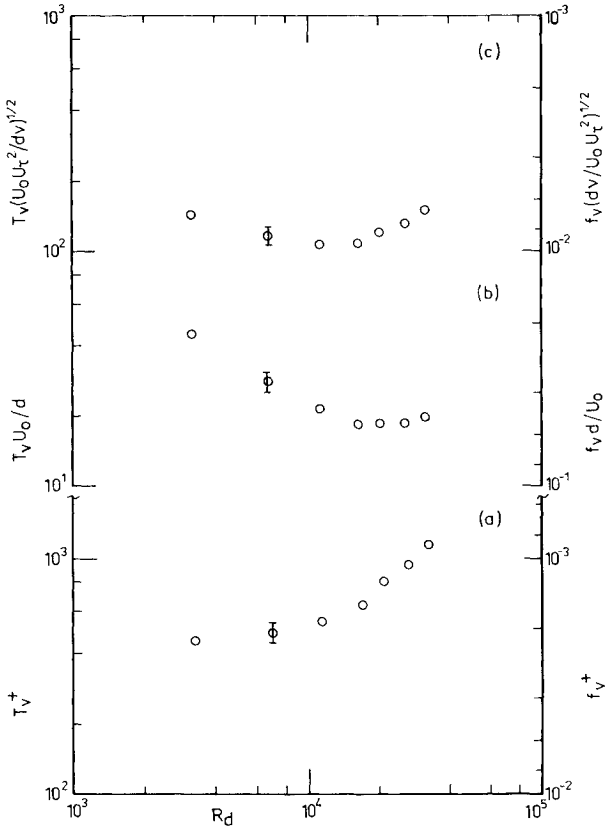

Fig. 4 Reynolds number dependence of the VITA detection frequency for $T^+ \simeq 13$: a) wall scaling; b) outer scaling; c) mixed scaling (vertical bar | indicates maximum uncertainty).

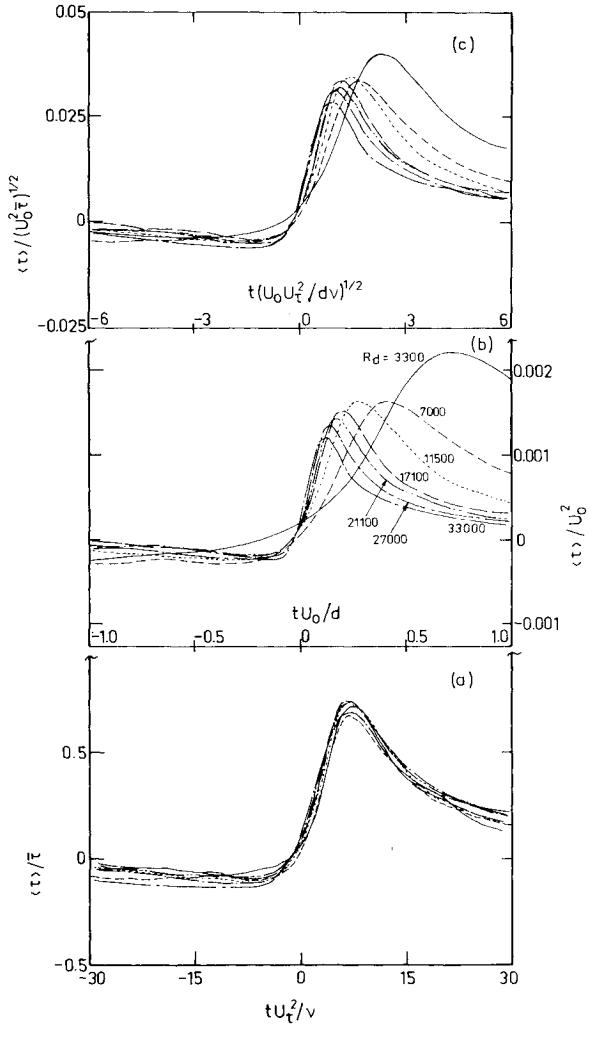

Fig. 5 Conditional averages, using VITA, of the wall shear stress for $T^+ \simeq 13$: a) wall scaling; b) outer scaling; c) mixed scaling.

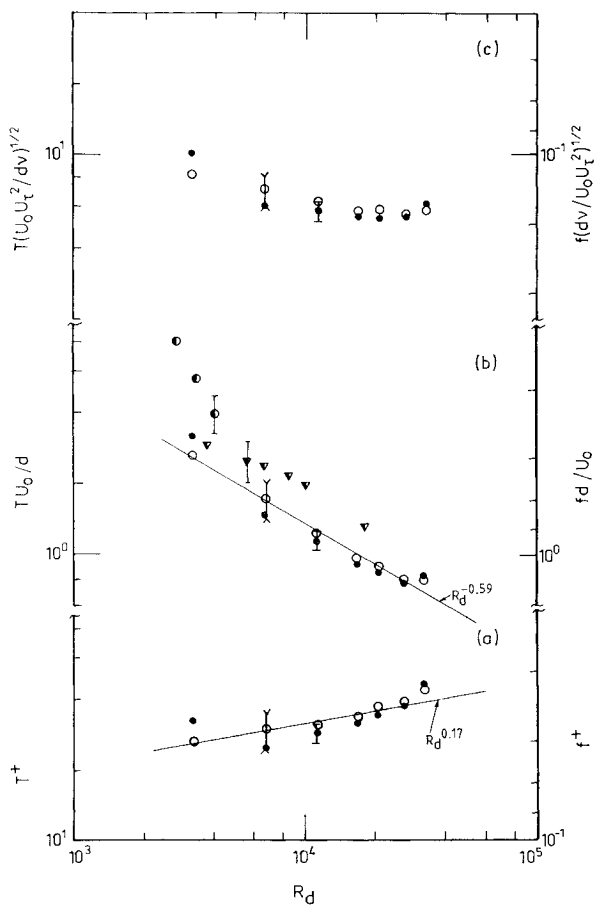

Fig. 6 Reynolds number dependence of the average zero-crossing frequency f_0 and of the average frequency of local maxima f_1: a) wall scaling; b) outer scaling; c) mixed scaling. Open and solid symbols are for f_0 and f_1, respectively; vertical bars ╳ and ╪ indicate maximum uncertainties in f_0 and f_1, respectively; • Eckelmann[25]; ▾ Sreenivasan and Antonia.[19]

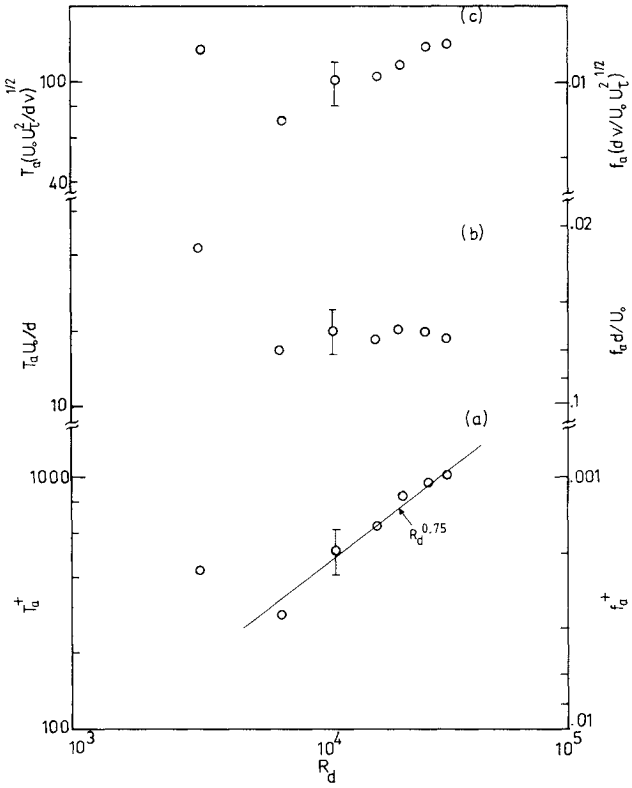

Fig. 7 Reynolds number dependence of the average frequency f_a: a) wall scaling; b) outer scaling; c) mixed scaling (vertical bar ╪ indicates maximum uncertainty).

Laufer and Badri Narayanan[18] with $T_a U_0/d \simeq 19(\pm 4)$ and $T_a^+ \sim R_d^{0.75}$ (Fig. 7).

Fleischmann and Wallace[39] found that the product of the mean period of organized structures, as obtained by different investigators using various techniques, and the convection velocity of these structures, is proportional to the shear layer thickness. This result, which was based on data for boundary-layer, pipe, and duct flows, was approximately independent of the Reynolds number or of the flow location at which the mean period is measured. The convection velocity, inferred from space-time correlations of shear stress fluctuations, has been shown[40] to be equal to about $0.5U_0$ for the present R_d range, asymptoting to $0.6U_0$ for $R_d > 35{,}000$. Fleischmann and Wallace's[39] proposal is therefore consistent with the outer scaling observed for the present measurements of T_v and T_a, but is not consistent with the scaling for T_0 or T_1.

When viewed in the context outlined by Fleischmann and Wallace,[39] outer scaling implies the existence of spatially coherent structures, perhaps in the form of hairpin eddies that, although stretched across the shear layer, can be detected at the wall. In support of this scenario is the reasonable agreement between the present values of f_v and those obtained, for the same VITA parameters, at several locations in the same flow.[14] For example, the present maximum value of $f_v d/U_0$, corresponding to $TU_0/d \simeq 0.8$, is about 0.11 for $R_d \gtrsim 21{,}100$. At $y^+ \simeq 15$ and $y/d = 0.5$, the corresponding values are 0.12 and 0.08. This type of agreement tends to suggest that VITA generally detects the same structures irrespective of location in the shear layer, corroborating the physical picture of Fleichmann and Wallace.[39] The decrease in the value of $f_v d/U_0$ at $y = 0.5d$ may reflect in part the likelihood that not all hairpin eddies will stretch across the full width of the shear layer.[39]

Conclusions

Estimates of the average frequency of detection obtained by applying several methods to the wall shear stress fluctuation, measured in a fully developed turbulent duct flow, indicate conflicting trends for the scaling of this frequency. The average frequencies inferred from VITA and from the autocorrelations suggest that scaling on either outer or mixed variables is more appropriate than scaling on inner variables. Results for the average frequency of zero-crossings and of local maxima rule out the possibility of outer scaling, but exhibit a definite (albeit weak) dependence on Reynolds number when inner scaling is used. We also have sufficient evidence to suggest that the same trends will be obtained when the different techniques considered here are applied to the longitudinal velocity fluctuation, irrespective of location in the shear layer. The disagreement between the present trend for the VITA detection frequency and that obtained in other investigations (e.g., Refs. 3 and 17) may be due to a failure, in these investigations, to account for genuine departures at insufficiently high Reynolds numbers from the Reynolds number similarity and for an insufficient spatial resolution of the sensors. In this context, it would clearly be desirable to extend the present investigation to a larger Reynolds number range. We should also emphasize that, unlike the results of Badri Narayanan et al.,[15] f_0 and f_1 exhibit nearly the same Reynolds number dependence. An analogous behavior for f_0 and f_1 is easy to reconcile with the close and physically plausible relationship that should exist between zero-crossings and local maxima of an instantaneous signal.

The apparent conflict between the Reynolds number trends of, on one hand, f_v or f_a and, on the other hand, f_0 or f_1, is not too surprising when viewed in the context of the relatively

complex interaction that presumably occurs between the inner and outer regions of the shear layer. The interaction is inherent in the bursting process and, in particular, the manner in which wall streaks interact with the outer region of the shear layer. The wall shear stress fluctuation exhibits a low-frequency component and a higher-frequency component with a strong likelihood of a coupling between these two (e.g., Refs. 27 and 41). It is reasonable to expect f_0 or f_1 to weight the higher-frequency part of the signal more strongly than the low-frequency part. In this sense, the stronger leaning in Fig. 6 on inner than on outer scaling is not surprising. By contrast, the stronger leaning in Fig. 4 on outer than on inner scaling reflects the emphasis given by VITA detections on structures that generally extend across the full width of the shear layer. Although VITA suffers from the disadvantages of one-point detection methods, there is a significant correlation between VITA detections and a characteristic feature associated with these structures (e.g., Ref. 8). The observation that the frequency f_a scales on outer variables (Fig. 7) reflects the weighting of the low-frequency part of the shear stress signal, presumably associated with these large structures via the second zero-crossing of the long-time autocorrelation.

The results of Figs. 4, 6, and 7 suggest that mixed variables may also be appropriate for scaling f_v, f_0 or f_1 and f_a. The evidence for this is not strong and even larger Reynolds numbers than could be considered here may be necessary before definite statements can be made. No clear physical meaning has been given to mixed scaling, except for the tentative suggestion by Alfredsson and Johansson[4] that this scaling reflects the interaction between the inner and outer regions. As noted earlier and, as discussed in Kline,[42] both the outer and inner regions are likely to be important to the dynamics of the flow. The geometric mean of inner and outer time scales is presumably only one of the different scalings of the mixed form that are possible. It would be unproductive to explore these possibilities until a firmer assessment can be made on the relative appropriateness of mixed and outer scaling, noting that outer scaling need not necessarily exclude the possibility of an interaction between the inner and outer regions.

Acknowledgments

We are grateful to Mr. L. V. Krishnamoorthy for his assistance with the construction of the wall shear stress probe. The support of the Australian Research Grants Scheme is gratefully acknowledged.

References

[1]Kim, H.T., Kline, S.J., and Reynolds, W.C., "The Production of Turbulence Near a Smooth Wall in a Turbulent Boundary Layer," *Journal of Fluid Mchanics*, Vol. 50, 1971, pp. 133-160.

[2]Narahari Rao, K., Narasimha, R., and Badri Narayanan, M.A., "The Bursting Phenomenon in a Turbulent Boundary Layer," *Journal of Fluid Mechanics*, Vol. 48, 1971, pp. 339-352.

[3]Blackwelder, R.F. and Haritonidis, J.H., "Scaling of the Bursting Frequency in Turbulent Boundary Layer," *Journal of Fluid Mechanics*, Vol. 132, 1983, pp. 87-103.

[4]Alfredsson, P.H. and Johansson, A.V., "Time Scales in Turbulent Channel Flow," *The Physics of Fluids*, Vol. 27, 1984, pp. 1974-1981.

[5]Badri Narayanan, M.A., Narasimha, R., and Narahari Rao, K., "Bursts in Turbulent Shear Flows," *Proceedings of Fourth Australasian Conference on Hydraulics & Fluid Mechanics*, Monash University, Melbourne, 1971, pp. 73-78.

[6]Offen, G.R. and Kline, S.J., "Combined Dye-Streak and Hydrogen Bubble Visual Observations of a Turbulent Boundary Layer," *Journal of Fluid Mechanics*, Vol. 62, 1974, pp. 223-239.

[7]Bogard, D.G. and Tiederman, W.G., "Investigation of Flow Visualization Techniques for Detecting Turbulent Bursts," *Proceedings of Seventh Biennial Symposium on Turbulence*, University of Missouri, Rolla, 1981, pp. 40-1-40-13.

[8]Subramanian, C.S., Rajagopalan, S., Antonia, R.A., and Chambers, A.J., "Comparison of Conditional Sampling and Averaging Techniques in a Turbulent Boundary Layer," *Journal of Fluid Mechanics*, Vol. 123, 1982, pp. 335-362.

[9]Hussain, A.K.M.F., "Coherent Structures—Reality and Myth," *The Physics of Fluids*, Vol. 26, 1983, pp. 2816-2850.

[10]Coles, D., "The Law of the Wake in the Turbulent Boundary Layer," *Journal of Fluid Mechanics*, Vol. 1, 1956, pp. 191-226.

[11]Head, M.R. and Bandyopadhyay, P., "New Aspects of Turbulent Boundary-Layer Structure," *Journal of Fluid Mechanics*, Vol. 107, 1981, pp. 297-338.

[12]Antonia, R.A., Chambers, A.J., and Bradley, E.F., "Relationships Between Structure Functions and Temperature Ramps in the Atmospheric Surface Layer," *Boundary-Layer Meteorology*, Vol. 23, 1982, pp. 395-403.

[13]Dean, R.B., "Reynolds Number Dependence of Skin Friction and Other Bulk Flow Variables in Two-Dimensional Rectangular Duct Flow," *Journal of Fluids Engineering*, Vol. 100, 1978, pp. 215-223.

[14]Shah, D.A., Antonia, R.A., and Chambers, A.J., "Scaling of the 'Bursting' Frequency in a Turbulent Duct Flow," Dept. of Mechanical Engineering, University of Newcastle, Australia, Rept. TN FM 84/12, 1984.

[15]Badri Narayanan, M.A., Raghu, S., and Poddar, K., "Wall Shear Fluctuations in a Turbulent Boundary Layer," *AIAA Journal*, Vol. 22, 1984, pp. 1336-1337.

[16]Johansson, A.V. and Alfredsson, P.H., "Effects of Imperfect Spatial Resolution on Measurements of Wall-Bounded Turbulent Shear Flows," *Journal of Fluid Mechanics*, Vol. 137, 1983, pp. 409-421.

[17]Chambers, F.W., Murphy, H.D., and McEligot, D.M., "Laterally Converging Flow. Part 2. Temporal Wall Shear Stress," *Journal of Fluid Mechanics*, Vol. 127, 1983, pp. 403-428.

[18]Laufer, J. and Badri Narayanan, M.A., "Mean Period of the Turbulent Production Mechanism in a Boundary Layer," *The Physics of Fluids*, Vol. 14, 1971, pp. 182-183.

[19]Sreenivasan, K.R. and Antonia, R.A., "Properties of Wall Shear Stress Fluctuations in a Turbulent Duct Flow," *Journal of Applied Mechanics*, Vol. 44, 1977, pp. 389-395.

[20]Bellhouse, B.J. and Schultz, D.L., "The Measurement of Fluctuating Skin Friction with Heated Thin-Film Gauges," *Journal of Fluid Mechanics*, Vol. 32, 1968, pp. 675-680.

[21]Baines, W.D. and Keffer, J.F., "Measurement of Shear Stress Near a Stagnation Point," *Review of Scientific Instruments*, Vol. 47, 1976, pp. 440-442.

[22]Ajagu, C.O., Libby, P.A., and LaRue, J.C., "Modified Gauge for Time-Resolved Skin-Friction Measurements," *Review of Scientific Instruments*, Vol. 53, 1982, pp. 1920-1926.

[23]Spence, D.A. and Brown, G.L., "Heat Transfer to a Quadratic Shear Profile," *Journal of Fluid Mechanics*, Vol. 33, 1968, pp. 753-773.

[24]Ramaprian, B.R. and Tu, S.W., "Calibration of a Heat Flux Gage for Skin Friction Measurement," *Journal of Fluids Engineering*, Vol. 105, 1983, pp. 455-457.

[25]Eckelmann, H., "The Structure of the Viscous Sublayer and the Adjacent Wall Region in a Turbulent Channel Flow," *Journal of Fluid Mechanics*, Vol. 65, 1974, pp. 439-459.

[26]Kreplin, H-P. and Eckelmann, H., "Behavior of the Three Fluctuating Velocity Components in the Wall Region of a Turbulent Channel Flow," *The Physics of Fluids*, Vol. 22, 1979, pp. 1233-1239.

[27]Thomas, A.S.W., "Organised Structures in the Turbulent Boundary Layer," Ph.D. Thesis, University of Adelaide, Australia, 1977.

[28]Badri Narayanan, M.A., Raghu, S., and Poddar, K., "Some Observations on the Instantaneous Structure of the Fluctuating Wall Shear in a Flat Plate Turbulent Boundary Layer," Dept. of Aerospace Engineering, Indian Institute of Science, Bangalore, India, Rept. 82FM15, 1982.

[29]Smith, C.R. and Metzler, S.P., "The Characteristics of Low-Speed Streaks in the Near-Wall Region of a Turbulent Boundary Layer," *Journal of Fluid Mechanics*, Vol. 129, 1983, pp. 27-54.

[30]Hogenes, J.H.A., "Identification of the Dominant Flow Structure in the Viscous Wall Region of a Turbulent Flow," Ph.D. Thesis, University of Illinois, Urbana-Champaign, 1979.

[31]Smith, C.R., "Visualization of Turbulent Boundary-Layer Structure Using a Moving Hydrogen Bubble-Wire Probe," *Coherent Structure of Turbulent Boundary Layers*, AFOSR/Lehigh University Workshop, 1978, pp. 48-97.

[32]Cantwell, B.J., "Organised Motion in Turbulent Flow," *Annual Review of Fluid Mechanics*, Vol. 13, 1981, pp. 457-515.

[33]Willmarth, W.W. and Sharma, L.K., "Study of Turblent Structure with Hot Wires Smaller than the Viscous Length," *Journal of Fluid Mechanics*, Vol. 142, 1984, pp. 121-149.

[34]Blackwelder, R.F. and Kaplan, R.E., "On the Wall Structure of the Turbulent Boundary Layer," *Journal of Fluid Mechanics*, Vol. 76, 1976, pp. 89-112.

[35]Johansson, A.V. and Alfredsson, P.H., "On the Structure of Turbulent Channel Flow," *Journal of Fluid Mechanics*, Vol. 122, 1982, pp. 295-314.

[36]Narasimha, R., "Comments on Blackwelden and Haritonidis 'Scaling of the Bursting Frequency in Subevident Boundary Layers'," Dept. of Aerospace Engineering, Indian Institute of Science, Bangalore, India, Rept. 83FM2, 1983.

[37]Zakkay, V., Barra, V., and Hozumi, K., "Turbulent Boundary Layer Structure at Low and High Subsonic Speeds," *Turbulent Boundary Layers—Experiments, Theory and Modelling*, AGARD CP-271, 1979, pp. 4-1-4-20.

[38]Sreenivasan, K.R., Prabhu, A., and Narasimha, R., "Zero-Crossings in Turbulent Signals," *Journal of Fluid Mechanics*, Vol. 137, 1983, pp. 251-272.

[39]Fleischmann, S.T. and Wallace, J.M., "Mean Streamwise Spacing of Organised Structures in Transitional and Developed Bounded Turbulent Flows," *AIAA Journal*, Vol. 22, 1984, pp. 766-769.

[40]Rajagopalan, S. and Antonia, R.A., "Some Properties of the Large Structure in a Fully Developed Turbulent Duct Flow," *The Physics of Fluids*, Vol. 22, 1979, pp. 614-622.

[41]Brown, G.L. and Thomas, A.S.W., "Large Structure in a Turbulent Boundary Layer," *The Physics of Fluids*, Vol. 20, 1977, pp. S243-S252.

[42]Kline, S.J., "The Role of Visualization in the Study of the Structure of the Turbulent Boundary Layer," *Coherent Structure of Turbulent Boundary Layers*, AFOSR/Lehigh University Workshop, 1978, pp. 1-27.